Supplementary Information

A general strategy to red-shift green fluorescent protein based biosensors

Shen Zhang and Hui-wang Ai*

Center for Membrane and Cell Physiology, Department of Molecular Physiology and Biological Physics, Department of Chemistry, and the UVA Cancer Center, University of Virginia, 1340 Jefferson Park Avenue, Charlottesville, Virginia 22908, United States

Correspondence should be sent to: huiwang.ai@virginia.edu

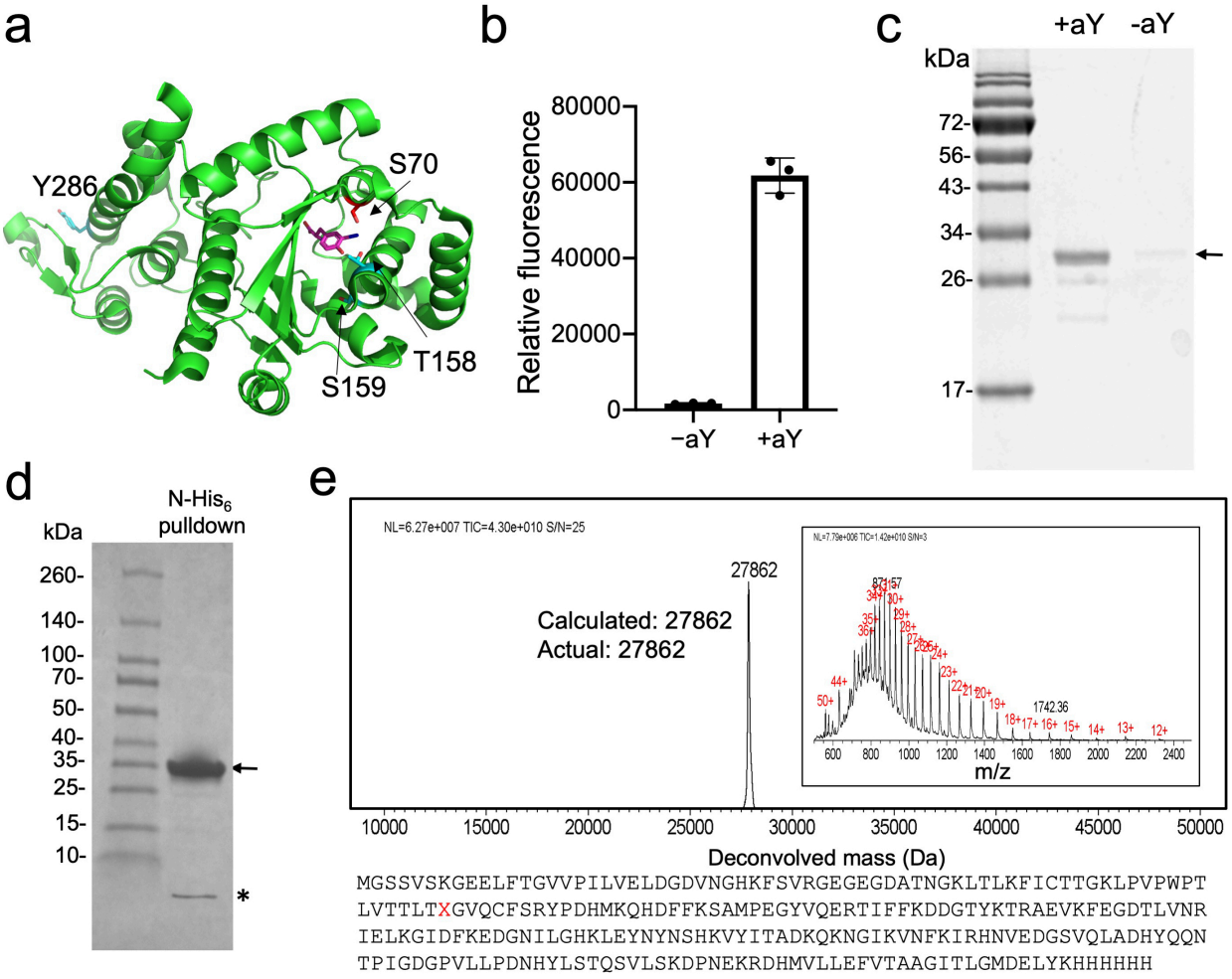

Supplementary Figure 1 Genetic encoding of 3-aminotyrosine (aY) in *E. coli*.

(**a**) Modeled structure of a *Methanococcus jannaschii* tyrosyl-tRNA synthetase mutant (*Mj*TyrRS-H70S/D158T/I159S/D286Y; a.k.a. *Mj*aYRS) in complex with aY. The template used for modeling is an *Mj*TyrRS mutant in complex with 3-iodotyrosine (Protein Data Bank 2ZP1).[1] This model was created with AutoDock Vina by following our previously reported procedure.[2] (**b**) Expression of pBAD-sfGFP(Tyr66TAG) with a C-terminal His_6 tag in the presence of pEvol-*Mj*aYRS, as indicated by relative red fluorescence of cell lysates in the presence or absence of aY. Data are presented as mean and s.d. of three independent replicates. (**c**) SDS-PAGE analysis of Ni-NTA-purified proteins (with a C-terminal His_6 tag) from *E. coli* in the presence or absence of aY. This experiment was repeated three times independently with similar results. (**d**) SDS-PAGE analysis of the Ni-NTA-purified protein (with a N-terminal His_6 tag) from *E. coli* in the presence aY, showing the full-length protein (indicated by the arrow) and a light band (indicated by the star) that might be the truncated protein (~ 7.9 kDa) caused by the incomplete suppression of the amber codon. This experiment was repeated twice with similar results. (**e**) ESI mass spectrometry analysis of the intact protein (with a C-terminal His_6 tag) purified from *E. coli* in the presence of aY and its respective amino acid sequence. The observed mass matched the calculated mass for sfGFP with aY at residue 66 (considering N-terminal Met cleavage, sfGFP chromophore maturation, and additional transformation to a mCherry-like chromophore). No peak corresponding to sfGFP with tyrosine at residue 66 (calculated mass: 27849 Da) was observed. The data collectively support that aY can be site-specifically introduced into proteins in *E. coli* by using our engineered aminoacyl-tRNA synthetase, *Mj*aYRS.

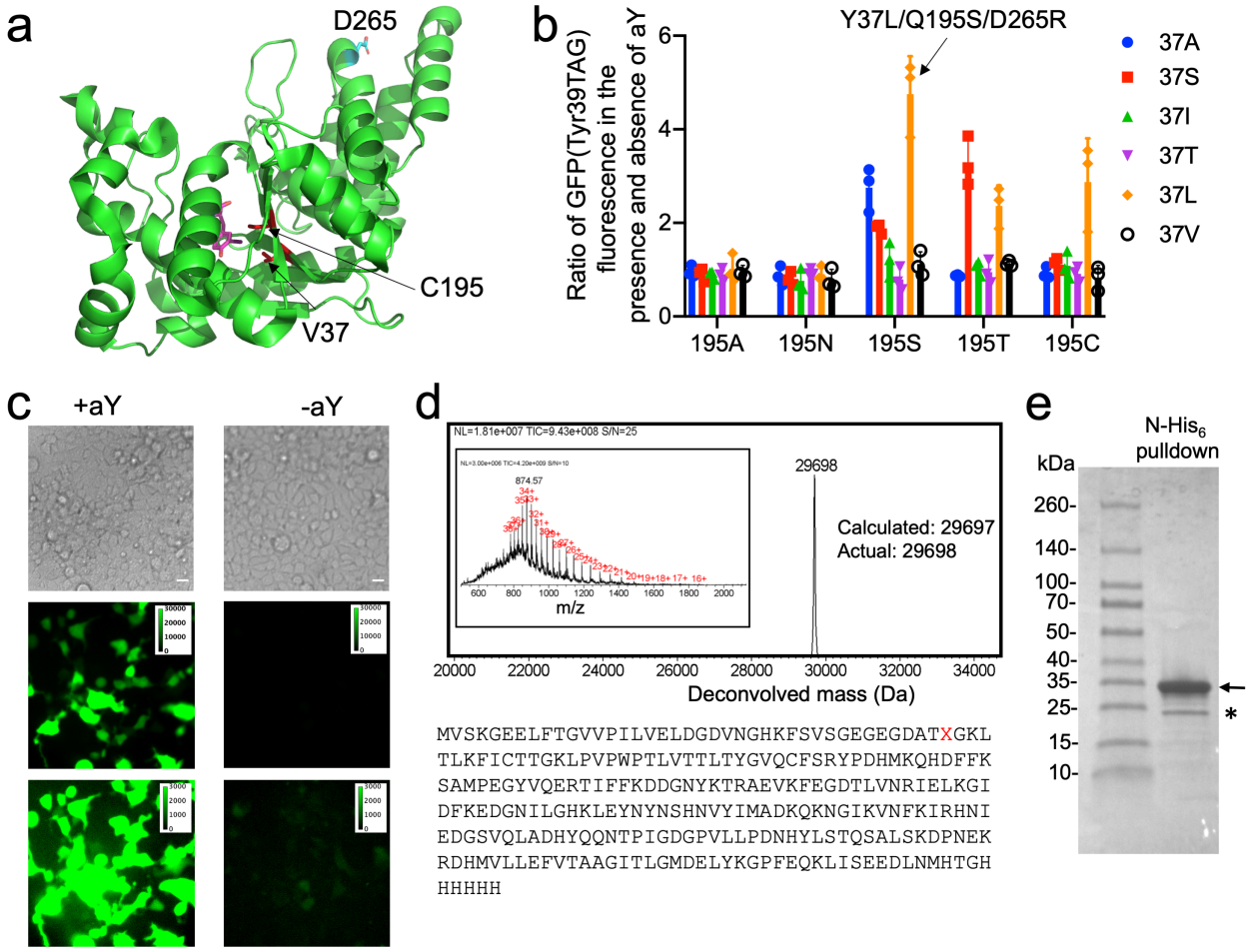

Supplementary Figure 2 Genetic encoding of 3-aminotyrosine (aY) in mammalian cells.

(**a**) Structure of an *E. coli* tyrosyl-tRNA synthetase mutant (*Ec*TyrRS-Y37V/Q195C) in complex with 3-iodotyrosine (Protein Data Bank 1WQ3). (**b**) Screening of *Ec*TyrRS mutants with mutations at residues 37 and 195 for the suppression of the amber TAG stop codon in pcDNA3-EGFP(Tyr39TAG) in HEK 293T cells. Data are presented as mean and s.d. of three independent replicates. A D265R mutation[3] and an additional tyrosine editing domain[4] were introduced into *Ec*TyrRS to derive *Ec*TyrRS*. A mutant (*Ec*TyrRS*-Y37L/Q195S/D265R) in pMAH was selected and named pMAH-*Ec*aYRS. (**c**) Microscopic imaging of HEK 293T cells transfected with pcDNA3-EGFP(Tyr39TAG) and pMAH-*Ec*aYRS in the presence (left column) or absence (right column) of aY (scale bar: 20 μm). Fluorescence images were presented twice with different intensity scales to show weak fluorescence in the absence of aY. This experiment was repeated three times independently with similar results. (**d**) ESI mass spectrometry analysis of intact EGFP (with a C-terminal His_6 tag) purified from HEK 293T cells in the presence of aY and its respective amino acid sequence. The difference between the observed and calculated masses for EGFP with aY at residue 39 is within the expected error range of the instrument. No peak corresponding to EGFP with tyrosine at residue 39 (calculated mass: 29682 Da) was observed. (**e**) SDS-PAGE analysis of the Ni-NTA-purified protein (with a N-terminal His_6 tag) from HEK 293T in the presence aY. The full-length protein is indicated by the arrow. The light band (indicated by the star) should be a contaminant. The truncated protein (~ 4.8 kDa) caused by the incomplete suppression of the amber codon was not observed, likely because it was unstable and degraded in HEK 293T. This experiment was repeated twice independently with similar results. The data collectively support that aY can be site-specifically introduced into proteins in mammalian cells by using our engineered aminoacyl-tRNA synthetase.

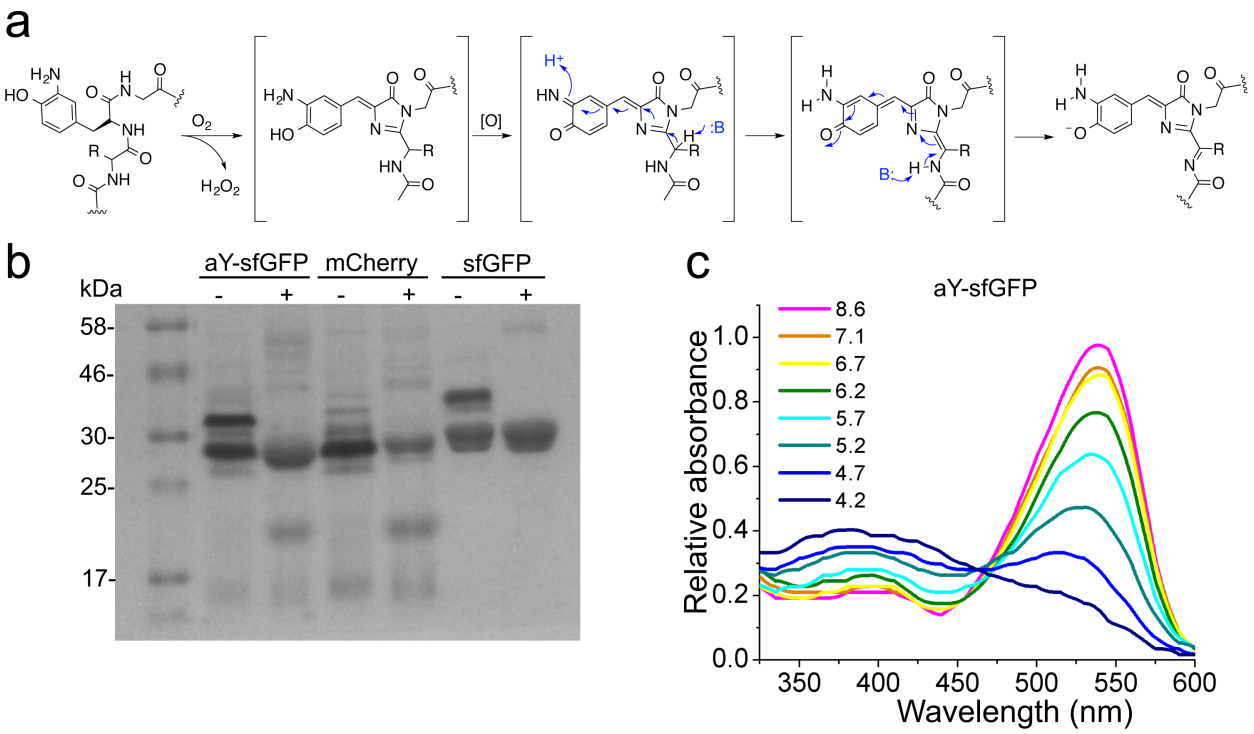

Supplementary Figure 3 Proposed chromophore transformations in GFP upon aY-modification of the chromophore.

(**a**) Proposed scheme for the conversion of the precursor polypeptide to the mature, red fluorescent chromophore. The formation of an mCherry-like chromophore is supported by polypeptide cleavage patterns in panel **b**. The negative charge of the chromophore is supported by pH titration in panel **c**. (**b**) Monitoring of polypeptide cleavage by SDS-PAGE. aY-sfGFP, mCherry, and sfGFP either unboiled (-) or boiled for 10 min (+) in 1x SDS gel-loading buffer were loaded to polyacrylamide gel. The boiled aY-sfGFP shows a polypeptide cleavage pattern similar to that of mCherry, suggesting the formation of a hydrolyzable C=N bond in aY-sfGFP. An additional band above 30 kDa was observed for both unboiled aY-sfGFP and sfGFP, likely due to additional folding states of these proteins. This experiment was repeated twice independently with similar results. (**c**) Absorbance of aY-sfGFP in response to pH changes. At low pH, the chromophore of aY-sfGFP is further protonated, as indicated by absorbance increase at ~ 400 nm.

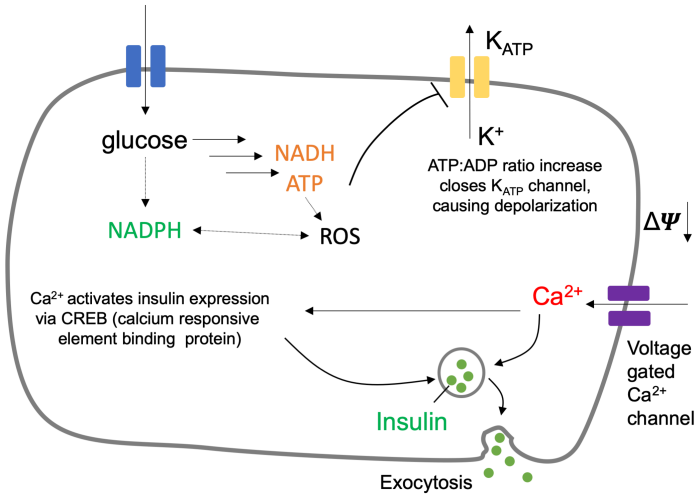

Supplementary Figure 4 Simplified metabolic model of glucose-stimulated insulin release from pancreatic β-cells.

NADH, ATP, NADPH, K^+, and Ca^{2+} are known coupling factors for glucose-stimulated insulin secretion.[5] In this simplified model, glucose is transported into β-cells through facilitated diffusion, is phosphorylated, and converted to substances such as pyruvate, NADH, NADPH, and ATP. ATP closes ATP-sensitive potassium (K_{ATP}) channels, initiating plasma membrane depolarization and increasing intracellular Ca^{2+} via voltage-dependent calcium channels (VDCCs). This glucose-induced cytosolic Ca^{2+} increase triggers the fusion of insulin granules with cell membrane and exocytosis of insulin, C-peptide, and a few other substances.

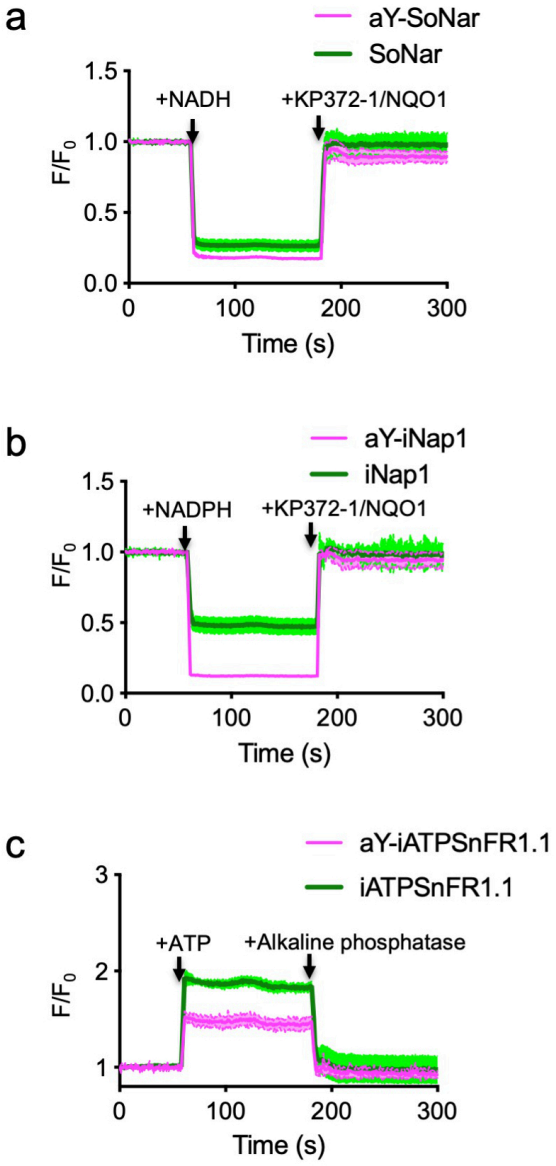

Supplementary Figure 5 Kinetics of fluorescence responses of the indicated biosensors.

(**a**) The responses of SoNar and aY-SoNar to the injection of 10 μM NADH, and then to the second injection of redox cycling agents containing 1.5 μM KP372-1 and 3 μM NQO1. (**b**) The responses of iNap1 and aY-iNap1 to the injection of 10 μM NADPH, and then to the second injection of redox cycling agents containing 1.5 μM KP372-1 and 3 μM NQO1. (**c**) The responses of iATPSnFR1.1 and aY-iATPSnFR1.1 to the injection of 500 μM ATP, and then to the second injection of 40 units of Thermo Scientific FastAP alkaline phosphatase. The measurements were done with a CLARIOstar Plus microplate reader (BMG Labtech) equipped with reagent dispensers. The observed kinetics was convoluted by the speed of reagent dispensing and mixing. Nevertheless, these fluorescence responses occurred and completed within a few seconds and were much faster than the time differences we discussed in our β-cell imaging experiments. Data are presented as mean and s.d. of three replicates.

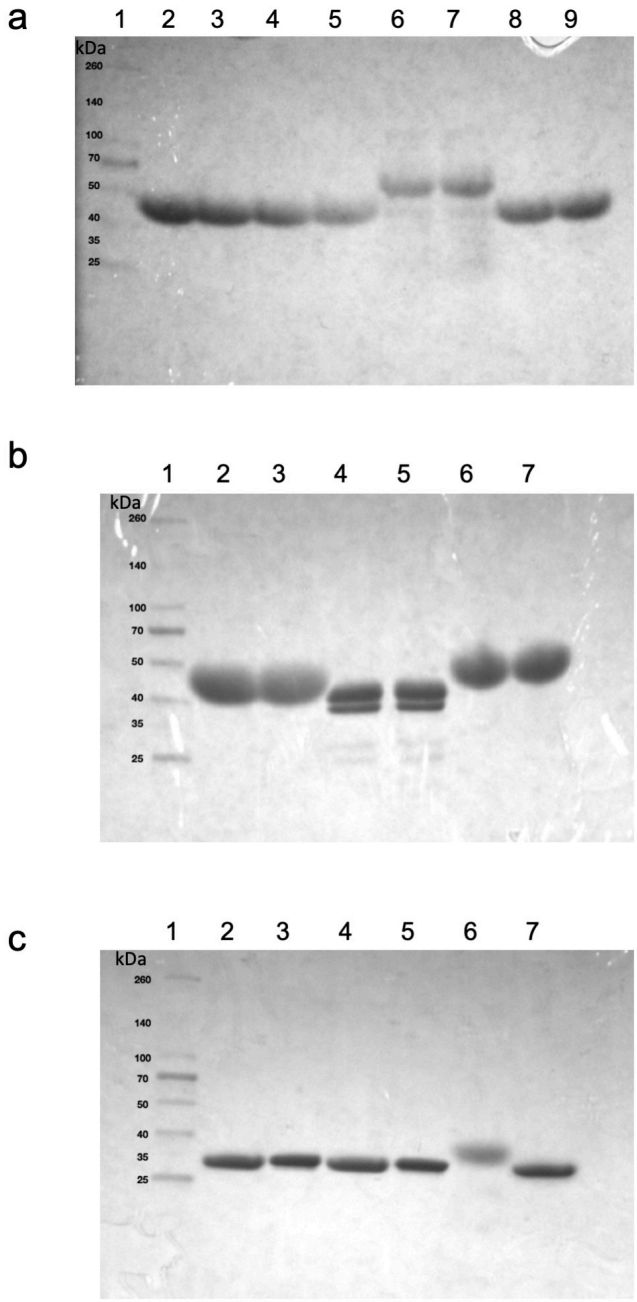

Supplementary Figure 6 SDS-PAGEs to show the purities of our prepared proteins.

Loaded to the first lane of each gel was Thermo Fisher Scientific Spectra™ Multicolor Broad Range Protein Ladder. Loaded to other lanes were purified proteins for (**a**) from lane 2 to lane 9: SoNar, aY-SoNar, iNap1, aY-iNap1, PercevalHR, aY-PercevalHR, iATPSnFR1.1 and aY-iATPSnFR1.1; (**b**) from lane 2 to lane 7: G-GECO1, aY-G-GECO1, ZnGreen1, aY-ZnGreen1, iGluSnFR and aY-iGluSnFR; (**c**) from lane 2 to lane 7: sfGFP, aY-sfGFP, aY-mTFP1, aY-cpYFP, aY-cpsGFP, and aY-Citrine. Two bands were observed for ZnGreen1 or aY-ZnGreen1, likely due to the proteins with and without Zn^{2+} ions pre-loaded in the *E. coli* host cells. These experiments were repeated twice independently with similar results.

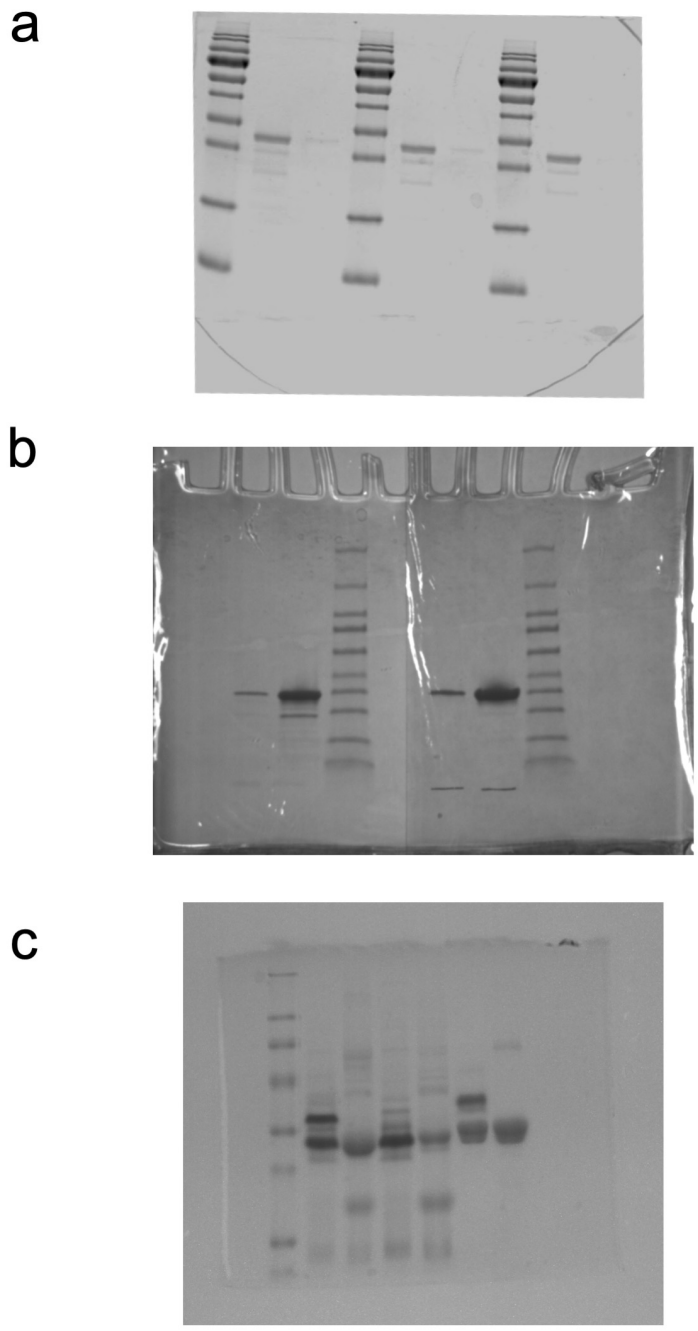

Supplementary Figure 7 Source data for supplementary figures.

Unprocessed gels for Supplementary Figures 1c (**a**), 1d and 2e (**b**), and 3b (**c**). In the background of the gel in panel **b** was a piece of folded white paper, thereby generating a line dividing the gel into two halves.

Supplementary Videos

Video 1. aY-G-GECO1 in HeLa cells in response to histamine, Ca^{2+}, and EGTA sequentially.

Video 2. aY-iGluSnFR and G-GECO1 in a mouse hippocampal neuron in response to high K^{+} depolarization.

Video 3. SoNar and Mito-aY-SoNar in MIN6 cells in response to high glucose.

References

1. Sakamoto K*, et al.* Genetic encoding of 3-iodo-L-tyrosine in Escherichia coli for single-wavelength anomalous dispersion phasing in protein crystallography. *Structure* **17**, 335-344 (2009).
2. Ren W, Truong TM, Ai HW. Study of the Binding Energies between Unnatural Amino Acids and Engineered Orthogonal Tyrosyl-tRNA Synthetases. *Sci. Rep.* **5**, 12632 (2015).
3. Takimoto JK, Adams KL, Xiang Z, Wang L. Improving orthogonal tRNA-synthetase recognition for efficient unnatural amino acid incorporation and application in mammalian cells. *Mol. BioSyst.* **5**, 931-934 (2009).
4. Oki K, Sakamoto K, Kobayashi T, Sasaki HM, Yokoyama S. Transplantation of a tyrosine editing domain into a tyrosyl-tRNA synthetase variant enhances its specificity for a tyrosine analog. *Proc. Natl. Acad. Sci. U. S. A.* **105**, 13298-13303 (2008).
5. MacDonald PE, Joseph JW, Rorsman P. Glucose-sensing mechanisms in pancreatic beta-cells. *Philos. Trans. R. Soc. Lond. B Biol. Sci.* **360**, 2211-2225 (2005).